Quantum Cellular Automata for Quantum Error Correction and Density Classification

T. L. M. Guedes,[*] D. Winter, and M. Müller
Institute for Quantum Information, RWTH Aachen University, D-52056 Aachen, Germany
and Peter Grünberg Institute, Theoretical Nanoelectronics, Forschungszentrum Jülich, D-52425 Jülich, Germany

(Received 15 September 2023; accepted 22 August 2024; published 7 October 2024)

Quantum cellular automata are alternative quantum-computing paradigms to quantum Turing machines and quantum circuits. Their working mechanisms are inherently automated, therefore measurement free, and they act in a translation invariant manner on all cells or qudits of a register, generating a global rule that updates cell states locally, i.e., based solely on the states of their neighbors. Although desirable features in many applications, it is generally not clear to which extent these fully automated discrete-time local updates can generate and sustain long-range order in the (noisy) systems they act upon. In particular, whether and how quantum cellular automata can perform quantum error correction remain open questions. We close this conceptual gap by proposing quantum cellular automata with quantum-error-correction capabilities. We design and investigate two (quasi)one dimensional quantum cellular automata based on known classical cellular-automata rules with density-classification capabilities, namely the local majority voting and the two-line voting. We investigate the performances of those quantum cellular automata as quantum-memory components by simulating the number of update steps required for the logical information they act upon to be afflicted by a logical bit flip. The proposed designs pave a way to further explore the potential of new types of quantum cellular automata with built-in quantum-error-correction capabilities.

DOI: 10.1103/PhysRevLett.133.150601

Introduction—Cellular automata (CAs) were proposed as simplified models of self-reproducing systems [1,2], but rapidly grew into powerful paradigms for the description of complex systems constructed from identical components with simple and local interactions [3]. Such emerging complexity renders CAs suitable candidates for computers [4], with proven universality [5,6] and reversibility (i.e., any irreversible CA can be simulated by a reversible CA) [7,8]. Error correction with CAs has been studied as a density-classification problem, i.e., whether a CA can force all cells of the system to the state that the majority of cells in any given initial configuration were in. It has been shown that no CA with two states per cell can perfectly classify the density when the number of cells is sufficiently large [9,10]. Nonetheless, a specific combination of CAs generates a perfect density classifier (DC) in the absence of noise [11,12], and certain CAs display formidable performances as DCs, even in the presence of noise [13–18].

Quantum cellular automata (QCAs), the quantum counterparts of CAs [19], were proposed as alternative universal quantum-computation models to quantum circuits and quantum Turing machines [20,21]. QCAs are defined axiomatically [22,23] and can be cast as local finite-depth circuits [24,25]. In QCAs, each cell is a quantum subsystem and the total system evolves unitarily in discrete time steps in a translation-invariant and quantum-locality-preserving (also called causal) manner [26–28]. This means that local operators are mapped into quasilocal operators at each step [25,29–31]. By implementing the evolution as an automorphism, QCAs can bypass the requirement of single- or few-qubit addressability, a prominent feature in proposals for experimental implementations of QCAs [32]. Even with QCAs making their way toward experimental realizations [33,34], it remains unclear if and how the quantum equivalent of the density-classification problem, quantum error correction (QEC), can be integrated in this framework, even though (classical) CAs have already been proposed to automatize syndrome analysis in QEC [35–43].

In this Letter, we study the density-classification performance under noise of two (quasi)1D CA rules, Wolfram's rule 232 [44] (also known as local majority voting), and Toom's two-line voting (TLV) [14]. We then propose QCAs corresponding to these rules and translate them into quantum circuits (cf. Fig. 1). Those are not only the first quantum-error-correcting (or quantum-DC) QCAs proposed, but, when concatenated, also proofs of the feasibility of QEC in or with QCA architectures. Their working principle is fundamentally different from usual QEC, since no measurements are needed [45–54]. Consequently, syndrome collection and classical decoding are absent, making our QCAs a fully quantum approach to QEC without quantum-to-classical interfaces. We simulate our QCAs' performances in the presence of coherent and incoherent phenomenological bit-flip noise, as well as

[*]Contact author: t.guedes@fz-juelich.de

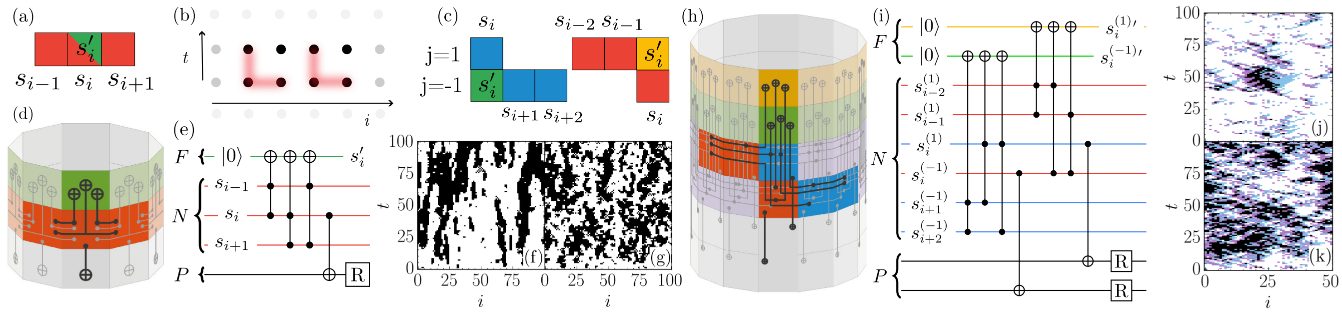

FIG. 1. Representations of Q232 (left) and QTLV (right). To guarantee reversibility, the QCAs are extended in one additional timelike dimension [vertical axes in the cylinders (d) and (h)], so that the global rule, shown as a combination of commuting and translation-invariant local unitaries U_i (colored), acts on the present register, covering an entire time-t section of the cylinder, while coupling to the future register (above) and decoupling from the past register (below). A single U_i (one for each j in the case of QTLV) is highlighted in each cylinder, showing how these local unitaries are decomposed into geometrically distributed parallelizable quantum gates, depicted in standard form in (e) for Q232 and (i) for QTLV, where P, N, F denote, respectively, past, present or now, and future, while R stands for reset. The classical neighborhood schemes N_d of the corresponding CAs are also highlighted in red [for Q232 in (d)] and blue and red [for QTLV in (h)], and they are also shown in isolated form in (a) and (c); in these representations, the future cells are shown in green (Q232) or green and yellow (QTLV) and their states are marked by primes. (f) and (j) show 232 and TLV orbits, respectively, under noise with bit-flip probability $p = 1/12$, while (g) and (k) show orbits when $p = 1/6$. In (j) and (k), each bistring is shown as a single string with four states: 00 (white), 01 (blue), 10 (purple), and 11 (black). Lastly, (b) represents schematically a potential Q232 realization in arrays of Rydberg atoms.

incoherent depolarizing circuit noise. Our simulations show that quantum two-line-voting (QTLV) is an excellent candidate for a quantum-memory component [55]. We compare the performances of our (Q)CAs to global voting, i.e., the classical repetition code [35], and show that under certain circumstances QTLV outperforms the repetition code [56,57]. We also briefly discuss some possibilities for experimental implementations of our QCAs. Lastly, we discuss how full QEC can be enabled through concatenation of our designs.

(Classical) Cellular automata—A deterministic d-dimensional CA, (L_d, S, f, N_d), is a system defined by a d-dimensional (often infinite) lattice L_d of identical cells, each having an internal set of states S and evolving according to a local function (rule) f mapping a neighborhood N_d of each cell into the update value of that cell [8]. A configuration over S (global state) is a map $\zeta\colon L_d \to S$, such that $\zeta(i) = s_i$ for the cell state s_i on site i. The set of all configurations is denoted $\mathrm{Conf}(S, L_d)$ and the global transition rule is a function $F\colon \mathrm{Conf}(S, L_d) \to \mathrm{Conf}(S, L_d)$. Space-time configurations generated by t applications of F on an initial configuration ζ, $F^{(t)}(\zeta) \equiv F\circ F\circ\ldots\circ F(\zeta)$, are called orbits [cf. Figs. 1(f), 1(g), 1(j), and 1(k)].

CA rules can be reversible or irreversible: every irreversible d-dimensional CA can be simulated by a reversible $(d+1)$-dimensional CA [7] and irreversible 1D CAs can always be simulated by some reversible 1D CA [8].

Although CAs cannot be perfect DCs [9,10], Ref. [11] showed that a combination of rules 184 and 232 in $(L_1 = \mathbb{Z}_n, S = \mathbb{Z}_2)$ systems generates a perfect DC. Rule 184, however, does not fulfill self-duality [35], what hinders the decoupling between different-time configurations in the corresponding QCA, as discussed later. We therefore initially focus on rule 232. We assume periodic boundary conditions throughout, since they best emulate the infinite-lattice scenario often encountered in CA and QCA theory and lead to superior performances in DCs. Other boundary conditions are also possible [35].

Rule 232 can be described as

$$s_i \to s_{i+1}s_{i-1} + s_{i+1}s_i + s_i s_{i-1} \mod 2 \tag{1}$$

and imprints on the central cell the majority (modulo 2) of all states $s_i \in \{0, 1\}$ in the neighborhood [see Fig. 1(a)]. As a noiseless DC, it can correct sole errors (e.g., a single state-1 cell in a background of state-0 cells or vice versa), and as long as sole errors are sparsely distributed throughout the lattice, successful density classification is possible. However, when errors group in the form of islands, rule 232 will map the latter into themselves, therefore making density classification impossible. This explains the poor performance of rule 232 under noise: whenever neighboring errors are created, density classification fails. In the presence of noise, 2- and 3-error islands have higher probabilities to grow than to shrink, while larger islands have similar probabilities for both cases. Therefore, over time the islands will contain over half of the cells [58].

A far more powerful quasi-1D ($\tilde{1}$D) DC, TLV, can be built from the 232 CA by extending the lattice to a double string, $L_{\tilde{1}} = \mathbb{Z}_{n/2} \oplus \mathbb{Z}_{n/2}$, and applying local majority voting, Eq. (1), with two different neighborhoods, each updating the cells on a different string [14] [cf. Fig. 1(c)]. Denoting the upper and lower string by superscripts $j = \pm 1$, TLV can be described as [cf. Fig. 1(c)]

$$s_i^{(j)} \to s_{i-j}^{(j)} s_{i-2j}^{(j)} + s_{i-j}^{(j)} s_i^{(-j)} + s_i^{(-j)} s_{i-2j}^{(j)} \mod 2. \quad (2)$$

In the absence of noise, it can be shown that every finite island of $2l+1$ errors on an infinite background of zeros or ones is eroded after a time $\leq ml$ for some CA-specific constant m, making TLV a linear eroder [15]. We show below that even with noise this property guarantees good performances.

Quantum cellular automata—A deterministic d-dimensional QCA is a system defined by a d-dimensional lattice Γ_d of identical cells, each of which has a Hilbert space $\mathcal{H}_i$ with a corresponding observable algebra $\tilde{\mathcal{A}}_i$ for $i \in \Gamma_d$. The QCA Hilbert space is $\mathcal{H} = \otimes_{i\in\Lambda} \mathcal{H}_i$ and its observable algebra is $\mathcal{A} = \otimes_{i\in\Lambda} \tilde{\mathcal{A}}_i$, where $\Lambda = \Gamma_d$ ($\Lambda \subset \Gamma_d$) for (in) finite Γ_d [25,59]. The QCA local operators are $a_i = \tilde{a}_i \otimes_{l\neq i} \tilde{\mathbb{1}}_l$ for $\tilde{a}_i \in \tilde{\mathcal{A}}_i$ and $l \in \Lambda$ and belong to the QCA local observable algebra $\mathcal{A}_i \cong \tilde{\mathcal{A}}_i$. The QCA evolves in time steps according to an automorphism (global rule) $u\colon \mathcal{A}_i \to \mathcal{A}_{\mathcal{R}_i}$ mapping local observables a_i of each cell i into quasilocal observables $a_{\mathcal{R}_i} \in \mathcal{A}_{\mathcal{R}_i} \cong \otimes_{l\in\mathcal{R}_i} \tilde{\mathcal{A}}_l$ acting nontrivially within some region $\mathcal{R}_i \subset \Gamma_d$ surrounding i [29,60] (note that an invertible map like u requires $\mathcal{A}_{\mathcal{R}_i}$ and $\mathcal{A}_i$ to cover the same set of cells, Λ). Besides being translation-invariant, u is locality-preserving, since it prevents the observables from spreading through the entire lattice in a single time step [61]. For finite lattices, $\exists\, U \in \mathcal{A}$ such that $u(a_i) = U^\dagger a_i U$. Lastly, there is a one-to-one correspondence (wrapping lemma [22]) between any translation-invariant QCA $(\Gamma_d, \mathcal{H}_i, \mathcal{A}_i, u, \mathcal{R}_i)$ on an infinite lattice and an equivalent QCA $(\Gamma'_d, \mathcal{H}_i, \mathcal{A}_i, u, \mathcal{R}_i)$ on a finite lattice with periodic boundary conditions. The two QCAs behave similarly provided that Γ'_d is sufficiently larger than $\mathcal{R}_i$ [62].

To achieve QCAs from the 232 and TLV CAs, we first make the latter reversible by encoding with F the time-$(t+1)$ configuration in a new (future) register while the time-t configuration remains stored in the present N register [7]. By keeping information from the states in the t and $(t+1)$ registers, one can construct reversible transition matrices that map $[s_{i_0,t}, s_{i_1,t}, s_{i_2,t}, s_{i_3,t+1}] \to [s_{i_0,t}, s_{i_1,t}, s_{i_2,t}, s_{i_3,t+1} + f(s_{i_0,t}, s_{i_1,t}, s_{i_2,t}) \mod 2]$ for time-t input cells $i_0, i_1, i_2 \in L_d$ whose states give through rule f the update $(t+1)$ value of cell i_3 [7,58]. In our case, f generates the transformations (1) and (2) for 232 and TLV, respectively, and for TLV i_0, i_1, i_2, i_3 also contain information about the location in the upper or lower strings. Such constructions can be seen as extensions of L_d to L_{d+1} with the additional dimension representing time [cf. Figs. 1(d) and 1(h)].

We consider each cell to be a qubit, and the QCAs to be started in an all-0 space-time configuration; the logical state is then encoded on the $t=0$ (bi)string. It turns out that self-duality in the CAs to be quantized, defined as $f(\neg s_{i-1}, \neg s_i, \neg s_{i+1}) = \neg f(s_{i-1}, s_i, s_{i+1})$, is a key property to allow for decoupling of past and present configurations. Self-duality means that two CA configurations ζ and $\bar{\zeta}$ with all cells in complementary states [i.e., $\zeta(i) = \bar{\zeta}(i) \oplus 1 \mod 2\ \forall\ i \in L_d$] will conserve this symmetry throughout their orbits, so that flipping all past cells of the orbit of $\bar{\zeta}$ makes all past configurations of ζ and $\bar{\zeta}$ the same. For a QCA constructed from a self-dual CA, that means that the present configuration can be kept as a coherent logical superposition of $|\zeta^{(t)}\rangle = \hat{E} \otimes_i |0_{i,t}\rangle$ and $|\bar{\zeta}^{(t)}\rangle = \hat{E} \otimes_i |1_{i,t}\rangle$, with some set of errors $\hat{E}$ on both, while past configurations are decoupled as a product state (which is the same for both logical states), $|\bar{\zeta}^{(t')}\rangle \to |\zeta^{(t')}\rangle$ for $t' < t$. It is worth noting that naive quantization of CAs often violates unitarity, translation invariance, locality and/or self-duality; the range of CA-derived 1D QCAs that perform QEC is therefore constrained. Hamiltonian systems, having continuous-time dynamics and generating generally nonlocal unitaries, cannot be QCAs [29,63,64].

The automorphism u can be built from a product of (quasi)local unitaries U_i associated with cells $i \in \mathcal{R}'_i \subseteq \mathcal{R}_i$ such that $U_i^\dagger(\cdot)U_i\colon \mathcal{A}_{\mathcal{R}'_i} \to \mathcal{A}_{\mathcal{R}'_i}$ [22]. In fact, to evolve the observables a_i it suffices to apply a product of a few U_j, since for $2i-j \notin \mathcal{R}'_i$ those unitaries act on the observable as the identity. $\mathcal{R}_i$ is then (contained in) the union of all $\mathcal{R}'_j$ such that $2i-j \in \mathcal{R}'_i$. For our quantized CAs, $\mathcal{R}'_i = N_{d+1}(i)$. In summary, $u(a_i) = (\prod_j U_j)^\dagger a_i (\prod_j U_j)|_{2i-j\in\mathcal{R}'_i}$ and, for finite Γ_d, $U = \prod_k U_k$. Such operator products are well defined only when $U_i U_k = e^{i\theta_{ik}} U_k U_i$ for some phase θ_{ik}, and therefore commuting unitaries are part of our QCA designs.

Quantum local majority voting (Q232)—The quantum version of rule 232, Q232, can be achieved by translating Eq. (1) into

$$U_{i,t} = (\sigma_{i,t-1}^{(x)})^{c_{i,t}} (\sigma_{i,t+1}^{(x)})^{[c_{i+1,t}c_{i-1,t} + c_{i+1,t}c_{i,t} + c_{i,t}c_{i-1,t}]} \quad (3)$$

for $c_{i,t} = [\mathbb{1}_{i,t} - \sigma_{i,t}^{(z)}]/2$. Note that $\sigma_{i,t}^{(x)} = \exp[\pm i\pi(\mathbb{1}_{i,t} - \sigma_{i,t}^{(x)})/2]$; therefore (3) can be expressed as an exponential operator. The $t+1$ operator in Eq. (3) can be decomposed into a product of three commuting Hermitian unitaries, one for each term in its exponent, each of which corresponds to a Toffoli gate. Similarly, the $t-1$ operator is a CNOT gate. We therefore see that the application of Q232 corresponds locally to three Toffoli gates and one CNOT per cell in the lattice, as shown in Figs. 1(d) and 1(e). The Toffoli gates are responsible for encoding into the future cell i the majority amongst the present-cell states in the neighborhood of i: $|s_{i-1,t}, s_{i,t}, s_{i+1,t}\rangle|0_{i,t+1}\rangle \to |s_{i-1,t}, s_{i,t}, s_{i+1,t}\rangle|s_{i,t+1}\rangle$ with $s_{i,t+1}$ given by the right-hand side of Eq. (1). The CNOTs make use of self-duality to decouple the past cells from the present and future ones. In this way, Q232 keeps a coherent logical superposition of $2n$ qubits. To recover the

n-qubit logical state or configuration, only the CNOTs are applied on the penultimate configuration. Similarly, given an initial logical state, the first application of Q232 uses only the Toffoli gates. One can also redefine Q232 so that the Toffoli gates are applied from $t \to t+1$ and the CNOTs afterward from $t+1 \to t$, so that a logical state of n qubits is kept at each time step.

Quantum two-line voting (QTLV)—By including an additional string-related superscript $j = \pm 1$ in Eq. (3), we derive the local-evolution unitary for QTLV,

$$U_{i,t}^{(j)} = (\sigma_{i,t-1}^{(x,j)})^{c_{i,t}^{(j)}} (\sigma_{i,t+1}^{(x,j)})^{[c_{i-j,t}^{(j)} c_{i-2j,t}^{(j)} + c_{i-j,t}^{(j)} c_{i,t}^{(-j)} + c_{i,t}^{(-j)} c_{i-2j,t}^{(j)}]}, \qquad (4)$$

with $c_{i,t}^{(j)} = [\mathbb{1}_{i,t}^{(j)} - \sigma_{i,t}^{(z,j)}]/2$. For each i, t and j, Eq. (4) can also be decomposed into three Toffoli gates and one CNOT [see Figs. 1(h) and 1(i)]. Since TLV works on two $n/2$-cell strings at each time step, QTLV acts on a total of six strings. One can, however, break each time step into two moves, one made of Toffoli gates ($t \to t+1$) and one made of CNOTs ($t+1 \to t$), so that a total of four strings are used. The global rule and locality-preserving properties of Q232 and QTLV are discussed in [58].

Simulation results—Having quantized the 232 and TLV CAs, we now quantitatively assess their QEC capabilities. We start with the original CAs. Figure 2 shows numerical evaluations of the average number of time steps (each corresponding to one application of noise followed by the CA rule [58]) necessary for the majority of cells of an all-0 initial configuration to be simultaneously found in state 1 (logical flip). We denote this quantity by flip time (FT). For each lattice size n and single-cell state-flip probability p, 10 000 orbits were sampled through Monte Carlo. For comparison, we also provide corresponding plots for global voting, applying noise $1+\Delta$ times before global readout and correction take place [58]. Since time is measured in CA steps, the global-voting operational time $1+\Delta$ accounts for a possible delay Δ. Figure 2(a) shows that for ten cells global voting with $\Delta = 2$ already underperforms TLV. Recent experimental realizations of the quantum repetition code showed measurement times at least 1 order of magnitude larger than gate-application times [57], so that $\Delta \gtrsim 5$ for realistic scenarios [58].

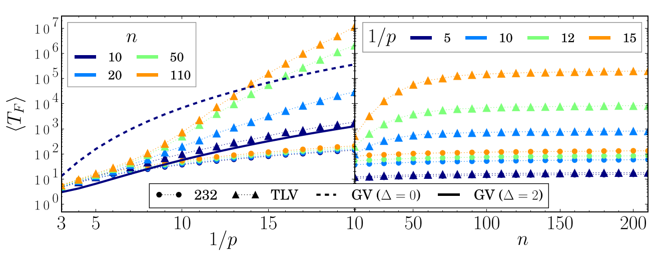

FIG. 2. (a) Numerical data for flip-time (FT) dependence on the inverse bit-flip probability per cell and time step, $1/p$, for several lattice sizes n (see color code). (b) FT dependence on n for certain fixed $1/p$ (color coded). The 232 and TLV FTs are represented by circular and triangular data points, respectively. Analytically derived FTs for global voting [58] with $n = 10$ and $\Delta = 0$ (dashed) or $\Delta = 2$ (solid) are also shown in (a).

One can see from Figs. 2(a) and 2(b) that the FTs for TLV surpass the 232 values for any n and p. The FT saturation in Fig. 2(b) results from CAs approaching the infinite-lattice behavior, as expected from the wrapping lemma. Locality prevents FTs from increasing unboundedly with n, evidencing the absence of phase transitions [29]. Furthermore, the FTs for TLV show a characteristic inflexion at $p \approx 1/8$. Our best fitting was achieved with $\langle T_F(p,n) \rangle = 2^{c_1 + \log_2^2(1/p)[f_1(n) + f_2(n)\tanh(c_2/p - c_3)]}$, with $f_i = a_i + b_i \exp(c_i n)$ as shown in [58]. This function interpolates between the two regimes separated by the inflexion and approximately reproduces the lower and upper bounds found in Ref. [15] for a similarly defined quantity.

We simulate the performances of Q232 and QTLV on PROJECTQ [65,66] via Monte Carlo sampling of 500 random orbits of $n = 12$ qubits per data point. We use a single future (bi)string of 12 additional qubits, so that at each time step, we encode the rule update on the future register, and then decouple future and present strings by applying CNOTs controlled by the future cells. We then reset the present string to an all-0 configuration and relabel strings according to "future" ↔ "present." We call flip time T_F the first time t at which $\sum_{i=1}^{n} \langle \sigma_{i,t}^{(z)} \rangle < 0$. The sequence of gates is maximally parallelized: each control and target qubit is acted upon by one single gate at each circuit step, leading to circuit depths of 7 for even n (cf. [58]). This design allows us to run Q232 and QTLV for a 12-qubit logical state using 24 qubits. The quantum circuits for the simulation of Q232 and QTLV are shown in [58]. We simulate our QCAs for different physical bit-flip probabilities applied both coherently and incoherently for the phenomenological model, and incoherent depolarizing noise for the circuit-noise model, as shown in Fig. 3.

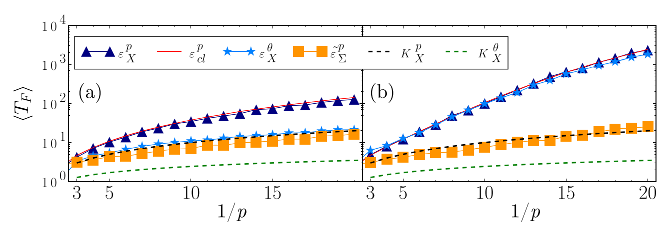

FIG. 3. Flip times of Q232 (a) and QTLV (b) as functions of $1/p$. Phenomenological incoherent and coherent [with $\sin^2(\theta/2) = p$] bit-flip noise are represented by blue triangles and stars, respectively; the corresponding noise channels are represented as ε_X^p and ε_X^θ. Circuit incoherent depolarizing noise corresponds to orange squares, with noise channel $\tilde{\varepsilon}_\Sigma^p$. For comparison, CA FTs are included as solid red curves (with channel ε_{cl}^p). FTs for incoherent (K_X^p) and coherent (K_X^θ) physical-qubit noise are included as dashed black and green lines, respectively, to show the absence of a pseudothreshold (no crossings with the QCA lines). See Ref. [58] for details.

We start with randomly generated logical states of the form $\cos(\phi) \otimes_i |0_{i,0}\rangle + i \sin(\phi) \otimes_i |1_{i,0}\rangle$ with $|\phi| < \pi/4$. We see from Fig. 3 that the performances of the QCAs coincide with CA ones when incoherent bit-flip noise is phenomenologically applied. Surprisingly, for phenomenological coherent noise, QTLV shows a considerably smaller performance drop relative to the incoherent model than the globally decoded quantum repetition code [56] (cf. Ref. [58]).

Concatenation—Both Q232 and QTLV can be concatenated to create QCAs capable of full QEC (i.e., correct both bit and phase flips). Just as the Shor code concatenates the repetition code in two complementary bases into a complete QEC code, we prove in Ref. [58] that a similar design for QTLV allows for improvement in FT of a logical state afflicted by bit and phase flips. Concatenation is therefore one path towards full QEC with our proposed QCAs.

Implementation proposal—Dynamically reconfigurable 2D arrays of neutral atoms allow for the parallelization of two- and three-qubit high-fidelity entangling gates [67–71]. The parallel gates required for our QCAs are therefore within experimental reach [58,72]. The reconfigurability of 2D neutral-atom arrays allows for rearrangement of time strings [68,69]. We expect Rydberg-atom platforms to be able to implement QCAs with globally applied locally conditional interactions [32,73] [cf. Fig. 1(b)], with trapped ions offering similar capabilities [74].

Conclusion—In this Letter, we introduce the first QCAs for QEC. These QCAs are reversible, translation-invariant, locality-preserving, self-dual, and independent from measurements and syndromes. They preserve coherence and information in the logical states they act upon while keeping errors local. Our simulation results highlight the robustness of QTLV, displaying remarkable performance against coherent and incoherent phenomenological noise. Our proposal for error-correcting QCAs opens the possibility to systematically explore and establish QCAs as a complementary paradigm for robust quantum information processing. We show that concatenation is one path toward QCA-based full QEC [58], yet higher-dimensional QCAs are also expected to have such capabilities. Topological properties of QCAs [29,75], potentially leveraging concepts from CAs and topological QEC [36–40], could lead to new approaches of QCA-based measurement-free QEC.

Acknowledgments—We thank K. Morita and P. Gács for fruitful discussions. We gratefully acknowledge support by the ERC Starting Grant QNets through Grant No. 804247. Furthermore, M. M. acknowledges support by the BMBF Project No. MUNIQC-ATOMS, the European Union's Horizon Europe research and innovation programme under Grant agreement No. 101114305 ("MILLENION-SGA1" EU Project). This research is also part of the Munich Quantum Valley (K-8), which is supported by the Bavarian state government with funds from the Hightech Agenda Bayern Plus. The authors gratefully acknowledge funding by the Deutsche Forschungsgemeinschaft (DFG, German Research Foundation) through Grant No. 449905436, and under Germany's Excellence Strategy "Cluster of Excellence Matter and Light for Quantum Computing (ML4Q) EXC 2004/1" 390534769. We acknowledge computing time provided at the NHR Center NHR4CES at RWTH Aachen University (Project No. p0020074). This is funded by the Federal Ministry of Education and Research and the state governments participating on the basis of the resolutions of the GWK for national high performance computing at universities.

[1] J. v. Neumann and A. W. Burks, *Theory of Self-Reproducing Automata* (University of Illinois Press, Urbana and London, 1966), http://www.arise.mae.usp.br/wp-content/uploads/2018/03/Theory-of-self-reproducing-automata.pdf.

[2] A. Adamatzky, *Game of Life Cellular Automata* (Springer, New York, 2010), Vol. 1, 10.1007/978-1-84996-217-9.

[3] S. Wolfram, Cellular automata as models of complexity, Nature (London) **311**, 419 (1984).

[4] S. Wolfram, Computation theory of cellular automata, Commun. Math. Phys. **96**, 15 (1984).

[5] A. R. Smith III, Cellular automata complexity trade-offs, Inf. Control **18**, 466 (1971).

[6] A. R. Smith III, Simple computation-universal cellular spaces, J. ACM **18**, 339 (1971).

[7] T. Toffoli, Computation and construction universality of reversible cellular automata, J. Comput. Syst. Sci. **15**, 213 (1977).

[8] K. Morita, Reversible simulation of one-dimensional irreversible cellular automata, Theor. Comput. Sci. **148**, 157 (1995).

[9] M. Land and R. K. Belew, No perfect two-state cellular automata for density classification exists, Phys. Rev. Lett. **74**, 5148 (1995).

[10] A. Bušić, N. Fatès, J. Mairesse, and I. Marcovici, Density classification on infinite lattices and trees, in *LATIN 2012: Theoretical Informatics*, edited by D. Fernández-Baca (Springer Berlin Heidelberg, Berlin, Heidelberg, 2012), pp. 109–120 [arXiv:1111.4582].

[11] H. Fukś, Solution of the density classification problem with two cellular automata rules, Phys. Rev. E **55**, R2081 (1997).

[12] J. R. G. Mendonça, Sensitivity to noise and ergodicity of an assembly line of cellular automata that classifies density, Phys. Rev. E **83**, 031112 (2011).

[13] P. Gács, G. L. Kurdyumov, and L. A. Levin, One-dimensional uniform arrays that wash out finite islands, Prob. Peredachi Inf. **14**, 92 (1978), https://www.mathnet.ru/links/85ef188c9b907bdd6ec60b20d3b4f288/ppi1551.pdf.

[14] A. Toom, Cellular automata with errors: Problems for students of probability, *Topics in Contemporary Probability and its Applications* (1995), p. 117.

[15] K. Park, Ergodicity and mixing rate of one-dimensional cellular automata, Ph.D. thesis, Boston University Computer Science Department, 1997, https://www.cs.bu.edu/faculty/gacs/papers/1996-015-park-phdthesis.pdf.

[16] P. Gács, Reliable computation with cellular automata, in *Proceedings of the Fifteenth Annual ACM Symposium on Theory of Computing* (1983), pp. 32–41, 10.1145/800061.808730.

[17] P. Gács, Reliable cellular automata with self-organization, J. Stat. Phys. **103**, 45 (2001).

[18] L. F. Gray, A reader's guide to Gacs's "positive rates" paper, J. Stat. Phys. **103**, 1 (2001).

[19] R. P. Feynman, Simulating Physics with Computers, in *Feynman and Computation* (CRC Press, Boca Raton, 2018), pp. 133–153.

[20] J. Watrous, On one-dimensional quantum cellular automata, in *Proceedings of IEEE 36th Annual Foundations of Computer Science* (1995), pp. 528–537, 10.1109/SFCS.1995.492583.

[21] D. J. Shepherd, T. Franz, and R. F. Werner, Universally programmable quantum cellular automaton, Phys. Rev. Lett. **97**, 020502 (2006).

[22] B. Schumacher and R. F. Werner, Reversible quantum cellular automata, arXiv:quant-ph/0405174.

[23] S. Richter and R. F. Werner, Ergodicity of quantum cellular automata, J. Stat. Phys. **82**, 963 (1996).

[24] P. Arrighi, V. Nesme, and R. Werner, Unitarity plus causality implies localizability, J. Comput. Syst. Sci. **77**, 372 (2011).

[25] P. Arrighi, An overview of quantum cellular automata, Nat. Comput. **18**, 885 (2019).

[26] P. Arrighi, C. Bény, and T. Farrelly, A quantum cellular automaton for one-dimensional QED, Quantum Inf. Process. **19**, 88 (2020).

[27] L. Mlodinow and T. A. Brun, Quantum field theory from a quantum cellular automaton in one spatial dimension and a no-go theorem in higher dimensions, Phys. Rev. A **102**, 042211 (2020).

[28] A. Bisio, G. M. D'Ariano, P. Perinotti, and A. Tosini, Free quantum field theory from quantum cellular automata: Derivation of Weyl, Dirac and Maxwell quantum cellular automata, Found. Phys. **45**, 1137 (2015).

[29] T. Farrelly, A review of quantum cellular automata, Quantum **4**, 368 (2020).

[30] C. A. Pérez-Delgado and D. Cheung, Local unitary quantum cellular automata, Phys. Rev. A **76**, 032320 (2007).

[31] J. Gütschow, S. Uphoff, R. F. Werner, and Z. Zimborás, Time asymptotics and entanglement generation of Clifford quantum cellular automata, J. Math. Phys. (N.Y.) **51** (2010).

[32] T. M. Wintermantel, Y. Wang, G. Lochead, S. Shevate, G. K. Brennen, and S. Whitlock, Unitary and nonunitary quantum cellular automata with Rydberg arrays, Phys. Rev. Lett. **124**, 070503 (2020).

[33] C. Huerta Alderete, S. Singh, N. H. Nguyen, D. Zhu, R. Balu, C. Monroe, C. Chandrashekar, and N. M. Linke, Quantum walks and Dirac cellular automata on a programmable trapped-ion quantum computer, Nat. Commun. **11**, 3720 (2020).

[34] E. B. Jones, L. E. Hillberry, M. T. Jones, M. Fasihi, P. Roushan, Z. Jiang, A. Ho, C. Neill, E. Ostby, P. Graf, E. Kapit, and L. D. Carr, Small-world complex network generation on a digital quantum processor, Nat. Commun. **13**, 4483 (2022).

[35] N. Lang and H. P. Büchler, Strictly local one-dimensional topological quantum error correction with symmetry-constrained cellular automata, SciPost Phys. **4**, 007 (2018).

[36] J. W. Harrington, *Analysis of Quantum Error-Correcting Codes: Symplectic Lattice Codes and Toric Codes* (California Institute of Technology, Pasadena, 2004).

[37] N. P. Breuckmann, K. Duivenvoorden, D. Michels, and B. M. Terhal, Local decoders for the 2D and 4D toric code, arXiv:1609.00510.

[38] A. Schotte, L. Burgelman, and G. Zhu, Fault-tolerant error correction for a universal non-Abelian topological quantum computer at finite temperature, arXiv:2301.00054.

[39] M. Herold, E. T. Campbell, J. Eisert, and M. J. Kastoryano, Cellular-automaton decoders for topological quantum memories, npj Quantum Inf. **1**, 15010 (2015).

[40] M. Herold, M. J. Kastoryano, E. T. Campbell, and J. Eisert, Cellular automaton decoders of topological quantum memories in the fault tolerant setting, New J. Phys. **19**, 063012 (2017).

[41] A. Kubica and J. Preskill, Cellular-automaton decoders with provable thresholds for topological codes, Phys. Rev. Lett. **123**, 020501 (2019).

[42] M. Vasmer, D. E. Browne, and A. Kubica, Cellular automaton decoders for topological quantum codes with noisy measurements and beyond, Sci. Rep. **11**, 2027 (2021).

[43] A. Ray, R. Laflamme, and A. Kubica, Protecting information via probabilistic cellular automata, arXiv:2304.03240.

[44] S. Wolfram, Statistical mechanics of cellular automata, Rev. Mod. Phys. **55**, 601 (1983).

[45] J. M. Gertler, B. Baker, J. Li, S. Shirol, J. Koch, and C. Wang, Protecting a bosonic qubit with autonomous quantum error correction, Nature (London) **590**, 243 (2021).

[46] H. E. Ercan, J. Ghosh, D. Crow, V. N. Premakumar, R. Joynt, M. Friesen, and S. N. Coppersmith, Measurement-free implementations of small-scale surface codes for quantum-dot qubits, Phys. Rev. A **97**, 012318 (2018).

[47] B. Cruikshank and K. Jacobs, High-threshold low-overhead fault-tolerant classical computation and the replacement of measurements with unitary quantum gates, Phys. Rev. Lett. **119**, 030503 (2017).

[48] G. A. Paz-Silva, G. K. Brennen, and J. Twamley, Fault tolerance with noisy and slow measurements and preparation, Phys. Rev. Lett. **105**, 100501 (2010).

[49] D. Crow, R. Joynt, and M. Saffman, Improved error thresholds for measurement-free error correction, Phys. Rev. Lett. **117**, 130503 (2016).

[50] P. M. Harrington, E. J. Mueller, and K. W. Murch, Engineered dissipation for quantum information science, Nat. Rev. Phys. **4**, 660 (2022).

[51] D. F. Locher, L. Cardarelli, and M. Müller, Quantum error correction with quantum autoencoders, Quantum **7**, 942 (2023).

[52] F. Carollo, M. Gnann, G. Perfetto, and I. Lesanovsky, Signatures of a quantum stabilized fluctuating phase and critical dynamics in a kinetically constrained open many-body system with two absorbing states, Phys. Rev. B **106**, 094315 (2022).

[53] M. A. Perlin, V. N. Premakumar, J. Wang, M. Saffman, and R. Joynt, Fault-tolerant measurement-free quantum error correction with multi-qubit gates, arXiv:2007.09804.

[54] S. Heußen, D. F. Locher, and M. Müller, Measurement-free fault-tolerant quantum error correction in near-term devices, PRX Quantum **5**, 010333 (2024).

[55] A. I. Lvovsky, B. C. Sanders, and W. Tittel, Optical quantum memory, Nat. Photonics **3**, 706 (2009).

[56] Y. Suzuki, K. Fujii, and M. Koashi, Efficient simulation of quantum error correction under coherent error based on the nonunitary free-fermionic formalism, Phys. Rev. Lett. **119**, 190503 (2017).

[57] Google Quantum AI, Exponential suppression of bit or phase errors with cyclic error correction, Nature (London) **595**, 383 (2021).

[58] See Supplemental Material at http://link.aps.org/supplemental/10.1103/PhysRevLett.133.150601 for details.

[59] It should be noted that an infinite tensor product of Hilbert spaces is an ill-defined construct. For this reason, the QCA Hilbert space can only be defined as $\mathcal{H} = \bigotimes_{i\in\Gamma_d} \mathcal{H}_i$ if Γ_d is finite. For an infinite lattice, the QCA Hilbert space has to be defined over sufficiently large regions Λ to allow for a description close to the infinite case. This is exactly the reason why QCA evolution is described in terms of automorphisms rather than unitaries. It is also the reason why a QCA description in terms of an alphabet Hilbert space makes use of (infinitely many) quiescent states to allow for a finite number of nonquiescent cell states composing a finite number of allowed configurations [25].

[60] P. Naaijkens, *Quantum Spin Systems on Infinite Lattices* (Springer, New York, 2013).

[61] In the language of QEC, this means that a physical error is not mapped into a logical error after a single time step.

[62] Namely, Γ'_d should be large enough relative to $\mathcal{R}_i$ that the intersection between overlapping neighborhoods of two cells in Γ_d, when one of them gets translated by some periods of Γ'_d, becomes empty.

[63] J. Zhang, G. Pagano, P. W. Hess, A. Kyprianidis, P. Becker, H. Kaplan, A. V. Gorshkov, Z.-X. Gonk, and C. Monroe, Observation of a many-body dynamical phase transition with a 53-qubit quantum simulator, Nature (London) **551**, 601 (2017).

[64] C. J. Turner, A. A. Michailidis, D. A. Abanin, M. Serbyn, and Z. Papić, Quantum scarred eigenstates in a Rydberg atom chain: Entanglement, breakdown of thermalization, and stability to perturbations, Phys. Rev. B **98**, 155134 (2018).

[65] D. S. Steiger, T. Häner, and M. Troyer, PROJECTQ: An open source software framework for quantum computing, Quantum **2**, 49 (2018).

[66] T. Häner, D. S. Steiger, K. Svore, and M. Troyer, A software methodology for compiling quantum programs, Quantum Sci. Technol. **3**, 020501 (2018).

[67] S. J. Evered *et al.*, High-fidelity parallel entangling gates on a neutral atom quantum computer, Nature (London) **622**, 268 (2023).

[68] D. Bluvstein *et al.*, A quantum processor based on coherent transport of entangled atom arrays, Nature (London) **604**, 451 (2022).

[69] D. Bluvstein *et al.*, Logical quantum processor based on reconfigurable atom arrays, Nature (London) **626**, 58 (2024).

[70] A. Browaeys and T. Lahaye, Many-body physics with individually controlled Rydberg atoms, Nat. Phys. **16**, 132 (2020).

[71] T. Graham *et al.*, Multi-qubit entanglement and algorithms on a neutral-atom quantum computer, Nature (London) **604**, 457 (2022).

[72] V. V. Shende and I. L. Markov, On the CNOT-cost of TOFFOLI gates, arXiv:0803.2316.

[73] H. Bernien *et al.*, Probing many-body dynamics on a 51-atom quantum simulator, Nature (London) **551**, 579 (2017).

[74] C. D. Bruzewicz, J. Chiaverini, R. McConnell, and J. M. Sage, Trapped-ion quantum computing: Progress and challenges, Appl. Phys. Rev. **6**, 021314 (2019).

[75] D. Gross, V. Nesme, H. Vogts, and R. F. Werner, Index theory of one dimensional quantum walks and cellular automata, Commun. Math. Phys. **310**, 419 (2012).